

been observed by Huang in Yb³⁺-doped diamagnetic garnets.²³ The T^2 dependence of our data is shown in Fig. 4.

ACKNOWLEDGMENTS

The authors would like to thank Dr. P. Bevington

for debugging advice about our computer programs. We are most grateful to Mrs. Su-Lee Huang for her data analysis; and to S. Lin and K. Sugawara for their crystal alignment.

¹D. A. Jones, J. M. Baker, and D. F. D. Pope, Proc. Phys. Soc. (London) **74**, 249 (1959).

²J. M. Baker and R. S. Rubens, Proc. Phys. Soc. (London) **78**, 1353 (1961).

³M. B. Schulz and C. D. Jeffries, Phys. Rev. **149**, 270 (1966).

⁴V. K. Sharma, Chem. Phys. Letters **4**, 545 (1970).

⁵I. Oftedal, Z. Physik. Chem. (Leipzig) **5B**, 272 (1929).

⁶I. Oftedal, Z. Physik. Chem. (Leipzig) **13B**, 190 (1931).

⁷K. Schlyter, Arkiv Kemi **5**, 73 (1953).

⁸M. Mansmann, Z. Anorg. Allgem. Chem. **331**, 98 (1964).

⁹M. Mansmann, Z. Krist. **122**, 375 (1965).

¹⁰A. Zalkin, D. H. Templeton, and T. E. Hopkins, Inorg. Chem. **5**, 1466 (1966).

¹¹J. H. Van Vleck and M. H. Hebb, Phys. Rev. **46**, 17 (1934).

¹²J. Becquerel, W. J. de Haas, and J. Van der Handel, Physica **1**, 383 (1934).

¹³R. P. Bauman and S. P. S. Porto, Phys. Rev. **161**, 842 (1967).

¹⁴R. P. Lowndes, J. F. Parrish, and C. H. Perry, Phys. Rev. **182**, 913 (1967).

¹⁵Optovac Inc., North Brookfield, Mass.

¹⁶C. A. Hutchison and E. Wong, J. Chem. Phys. **29**, 754 (1958).

¹⁷R. C. Mikkelsen and H. J. Stapleton, Phys. Rev. **140**, A1968 (1965).

¹⁸R. J. Elliot and K. W. H. Stevens, Proc. Roy. Soc. (London) **A215**, 437 (1952).

¹⁹A. H. Cooke and J. G. Park, Proc. Phys. Soc. (London) **A69**, 282 (1956).

²⁰P. R. Bevington, *Data Reduction and Error Analysis for Physical Sciences* (McGraw-Hill, New York, 1969).

²¹H. H. Caspers, H. E. Rast, and R. A. Buchanan, J. Chem. Phys. **42**, 3214 (1965).

²²E. V. Sagre and Simon Freed, J. Chem. Phys. **23**, 2066 (1955).

²³Chao-Yuan Huang, Phys. Rev. **139**, A241 (1965).

Energy Distributions for Thermal Field Emission

J. W. Gadzuk and E. W. Plummer

National Bureau of Standards, Washington, D. C. 20234

(Received 16 November 1970)

A sequence of total energy distribution curves for field emission was experimentally obtained for a tungsten emitter heated to 1570 K. Theoretical curves using the Miller-Good WKB-type approximation for tunneling probabilities are in good agreement with the experimental measurements. A significant feature of both sets of curves is a change in slope corresponding to electron emission near the top of the surface barrier where the emission mechanism changes from tunneling to thermionic emission. This feature is in accord with the classical-image force model for the surface potential which appears to be valid for distances approaching 3–4 Å to the metal surface.

I. INTRODUCTION

Measurement of the total energy distribution (TED) of field-emitted electrons¹ is becoming an increasingly powerful method for obtaining information on electron states in and on metals. For instance, studies both experimental^{2,3} and theoretical⁴ on band-structure effects, virtual electron states in chemisorbed atoms,^{3,5} electron-electron interactions,⁶ and *d*-band metal surface states^{7,8} have proven to be useful in furthering the understanding of the electronic properties of the materials investigated, and have shown the versatility of the field-emission technique. In this paper we

present the first detailed experimental data and analysis of thermal field-emission TED curves in which the details of the surface barrier result in observable and predictable structures in the TED.

II. EXPERIMENT

The experimental measurements were made using a Kuyatt-Simpson-type spherical deflection energy analyzer.⁹ The inherent thermal noise in a field emitter² was overcome by appropriate signal averaging, using a multichannel analyzer. The field emitter was dc heated at 1570 K (measured by an optical pyrometer) in the presence of an electric field for many hours prior to making a measure-

ment in order to stabilize the emitter end form. As a consequence of this prolonged heating, a noticeable carbon contamination built up on the tip which raises the work function¹⁰ above 4.4 eV. There was no noticeable contamination from the ambient gases at the pressure of 10^{-11} Torr during a measurement.

III. THEORY

The total energy distribution of field-emitted electrons from a free-electron metal is schematically shown in Fig. 1 and given by

$$j'(\epsilon) = (4\pi me/h^3) f(\epsilon) \int_0^{\epsilon + E_F} D(W) dW, \quad (1)$$

with $\epsilon = E - E_F$, E_F the Fermi energy measured with respect to the zero of kinetic energy at the bottom of the conduction band, and $f(\epsilon) = (1 + e^{\epsilon/kT})^{-1}$, the Fermi function.¹ The tunneling or transmission function $D(W)$ is integrated over all energetically allowed values of W , the "normal energy," or value of kinetic energy associated with the component of momentum perpendicular to the surface. As discussed elsewhere,⁴ the drastically reduced tunneling probabilities for d -band electrons compared to s -like electrons play down any dramatic d -band density-of-states effects one might expect in transition metals. Consequently, no explicit reference to density of states is required here. This study is concerned with emission near the top of the surface potential barrier formed by the image potential plus applied field, $V(z) = -e^2/4z - eFz$, as shown in Fig. 1. In this case, the usual WKB approximation to the tunneling probability together with a Taylor series expansion of the WKB result around the Fermi energy does not provide an adequate description of the tunneling process.¹⁰ Consequently, the barrier penetration function obtained in the WKB-like approximation of Miller and Good, which is valid for electrons of all relevant energies, is

used¹¹⁻¹⁵:

$$D(W) = [1 + e^{A(W)}]^{-1}. \quad (2)$$

The phase integral in Eq. (2) is given by

$$A(W) = 2 \int_{z_1}^{z_2} \left[\frac{2m}{\hbar^2} \left(\varphi + E_F - eFz - \frac{e^2}{4z} - W \right) \right]^{1/2} dz,$$

with z_1 and z_2 the turning points obtained as the roots of the integrand set equal to zero.

For thermal field emission near the top of the barrier where $E_m = \varphi + E_F - (e^3 F)^{1/2} = \varphi + E_F - 3.79 F^{1/2}$ with F in $V/\text{\AA}$, the detailed shape of the barrier is important in determining the shape of the TED. Therefore, the phase integral $A(W)$ in Eq. (2) must be expressed in terms of the standard elliptic integrals as discussed by Good and Müller,¹⁰ and thus

$$A(W) = \frac{4}{3} \left(\frac{2m}{\hbar^2} \right)^{1/2} \frac{(E_F + \varphi - W)^{3/2}}{eF} v \left(\frac{(e^3 F)^{1/2}}{E_F + \varphi - W} \right), \quad (3)$$

where $v(y)$ is the tabulated elliptic function accounting for the curvature of the tunneling barrier due to the image potential.¹⁰ Equations (2) and (3) are inserted in Eq. (1) which in turn must be numerically integrated to obtain values for the thermal TED.

IV. RESULTS

The results for a sequence of $T = 1570$ K TED's are shown in Figs. 2(a) and 2(b). Figure 2(a) displays the experimentally measured results for a series of emitter-to-anode voltages corresponding to electric fields at the tip ranging from ~ 0.08 to 0.4 $V/\text{\AA}$. Voltage has been taken as the variable parameter rather than field because of inherent ambiguity in field determinations in field-emission experiments.¹⁶ In Fig. 2(b), the numerical values of

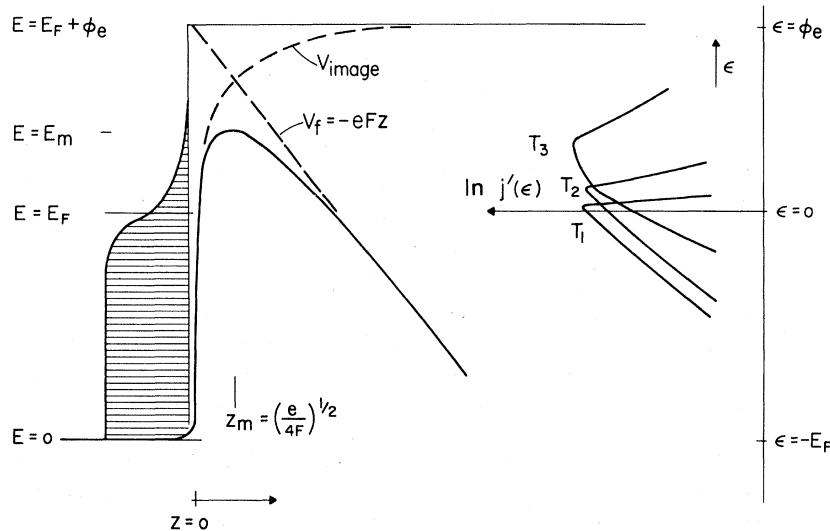


FIG. 1. Model potential at a metal surface during a field-emission event together with $\ln j'$ vs ϵ for temperatures $T_1 < T_2 < T_3$. The total surface barrier is the sum of the image potential V_{image} plus the applied field.

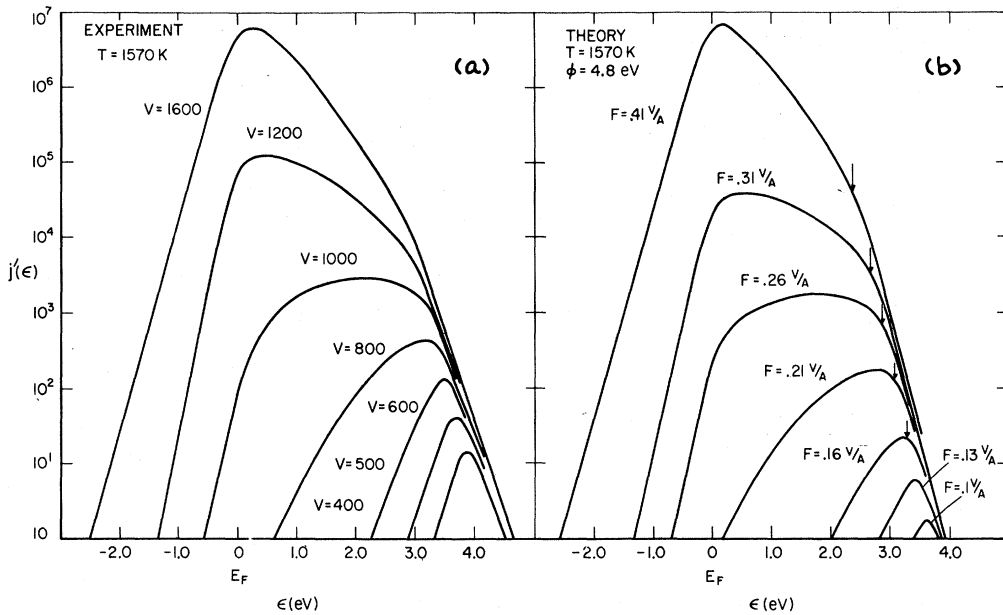


FIG. 2. (a) Experimental TED with emitter-to-anode voltage varied parametrically for $T = 1570$ K. (b) Theoretical TED with field treated parametrically for $\phi = 4.8$ eV and $T = 1570$ K. The units of j' are arbitrary.

the TED calculated from Eqs. (1)–(3) are shown. The theoretical fields are calculated to be consistent with the slope of the experimental Fowler-Nordheim plot and the assumed work function. We have taken $E_F = 8$ eV and $T = 1570$ K. A choice of work function $\phi = 4.8$ eV gives the best over-all coincidence between theory and experiments.

As seen in Figs. 2(a) and 2(b), the similarity between experiment and theory is good. Three distinct regions in the TED are to be noted: exponentially decaying tails at (i) low energies with slope $1/d$, (ii) high energies with slope $-1/kT$, displaying, respectively, the usual tunneling probability for electrons with energies near the Fermi energy and the Boltzmann tail of the Fermi function, (iii) the intermediate transition region in which the slope is either positive or negative depending upon the values of field and temperature but always with a distinct change of log slope near the barrier top $\epsilon = E_m - E_F$. The value of $E_m - E_F$ marked by arrows in Fig. 2(b), seems to be experimentally significant. From image-potential theories, the barrier maximum occurs at a distance $z_m = (e/4F)^{1/2} = 1.9/F^{1/2}$ Å from the surface where F is in units of $V/\text{\AA}$ and z_m in Å. Both E_m and z_m depend upon the accuracy of the image-type approximation, and since experimental values of E_m are consistent with the value of E_m obtained from an image-potential picture, the results presented here suggest that image-potential theories should be meaningful, even to distances $z_m \approx 3\text{--}4$ Å from metal surfaces. This is the order of electron-metal separation which Sachs and Dexter suggest may result in the breakdown of the image potential due to

other quantum-mechanical effects.¹⁷ Studies of such effects as periodic Schottky deviations have also shown that the image potential is reasonable, but only for electron-metal separations at least an order of magnitude greater than the values in the present study.¹⁸ Although the uniqueness of the image-potential approximation to the surface potential has not been proven, its utility for the TED has been displayed. To our knowledge, this is the most direct study demonstrating the implications of surface-potential shapes at such small distances from the metal surface and provides a striking confirmation of the image potential at a metal surface.

The necessity of using the full analytic form of the tunneling probability including image force corrections and no expansions about the Fermi energy when interpreting TED ranging over several eV has also been established. From a theoretical point of view, we have also displayed the utility and general reasonableness of the Miller-Murphy-Good WKB-like approximation for describing tunneling near the top of a barrier.

V. RELATION TO PAST WORK

The widely used expression for the TED which results from making the WKB approximation and an expansion of $A(W)$ about $W = E_F$ is

$$j'_0(\epsilon) = (J_0/d) f(\epsilon) e^{\epsilon/d}, \quad (4)$$

with

$$J_0 = \frac{4\pi m e}{h^3} d^2 e^{-c},$$

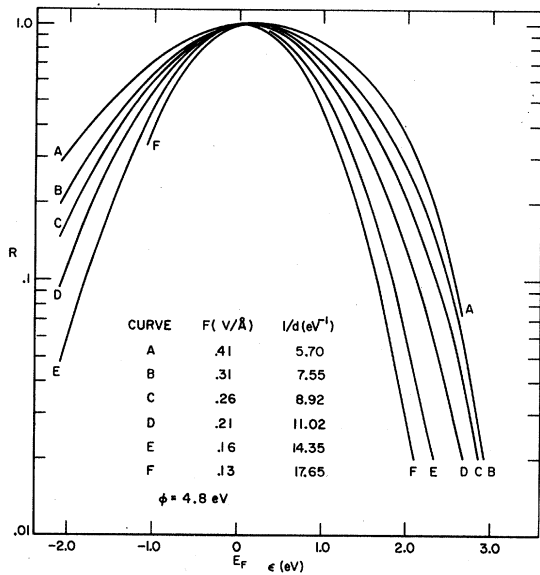


FIG. 3. Ratio of "exact" to expansion tunneling probability as a function of energy from the Fermi level. Field and thus $1/d = 1.025 (\varphi/F)^{1/2} t (3.79 F^{1/2}/\varphi) \text{ eV}^{-1}$ are treated parametrically. Here, φ is in units of eV and F in V/Å.

$$\begin{aligned}
 c &= \frac{4}{3} \left(\frac{2m}{\hbar^2} \right)^{1/2} \frac{\varphi^{3/2}}{eF} v \left(\frac{(e^3 F)^{1/2}}{\varphi} \right) \\
 &= \frac{0.68 \varphi^{3/2}}{F} v \left(\frac{3.79 F^{1/2}}{\varphi} \right), \\
 \frac{1}{d} &= 2 \left(\frac{2m}{\hbar^2} \right)^{1/2} \frac{\varphi^{1/2}}{eF} t \left(\frac{(e^3 F)^{1/2}}{\varphi} \right) \\
 &= \frac{1.025 \varphi^{1/2}}{F} t \left(\frac{3.79 F^{1/2}}{\varphi} \right) \text{ eV}^{-1},
 \end{aligned}$$

and $t(y) = v(y) - \frac{2}{3} y dv(y)/dy$.^{1,10} The simple algebraic expression Eq. (4) fairly accurately repro-

duces the low-temperature experimental TED for energies within ~ 0.5 eV of the Fermi energy provided no band-structure or surface-state effects are important.^{3,4,8}

To illustrate this point consider Fig. 3 where the quantity $R(\epsilon) = j'(\epsilon)/j'_0(\epsilon)$ is displayed for several different values of field. Values for $j'(\epsilon)$ were obtained by numerically integrating Eq. (1) using Eqs. (2) and (3). As can be seen, the value of R , which is also just the ratio of "exact" to expansion tunneling probabilities, is close to unity only within a few tenths of an eV of the Fermi energy. Rather surprisingly, the value of R is very close to unity, within the width of the lines on the graph, for $\epsilon = 0$. This just indicates how strongly the $\epsilon = 0$ emission is dominated by electrons with normal energies in the narrow range $E_F - d \lesssim E \lesssim E_F$ in the integral of Eq. (1).

Because past energy-analysis experiments measured electron emission only within about 0.5 eV of E_F , the simplified $j'_0(\epsilon)$ provided a reasonable correlation with data.¹⁻³ Some deviations from the expansion TED which could be explained by including higher-order terms in the expansion of the tunneling probability about the value of E_F were noted by Plummer and Young.³ Experiments which measure the integrated distribution or total current equal to J_0 (at zero temperature) are the least sensitive to the types of corrections pointed out here, since most of the emission comes from energy levels right at E_F where $R \approx 1$.¹⁹ However, with the advent of new analyzers which are increasing the working range of energies by about a factor of 4, much closer attention will have to be paid to the details of the tunneling barrier as has been done here.

ACKNOWLEDGMENT

We thank B. Waclawski for careful readings and constructive comments pertaining to this manuscript.

¹R. D. Young, Phys. Rev. **113**, 110 (1959); R. D. Young and E. W. Müller, *ibid.* **113**, 115 (1959); J. W. Gadzuk, Surface Sci. **15**, 466 (1969).

²L. W. Swanson and L. C. Crouser, Phys. Rev. Letters **16**, 389 (1966); Phys. Rev. **163**, 622 (1967).

³E. W. Plummer and R. D. Young, Phys. Rev. B **1**, 2088 (1970).

⁴J. W. Gadzuk, Phys. Rev. **182**, 416 (1969); D. Nagy and P. H. Cutler, *ibid.* **186**, 651 (1969); B. A. Politzer and P. H. Cutler, Mater. Res. Bull. **5**, 703 (1970).

⁵J. W. Gadzuk, Phys. Rev. B **1**, 2110 (1970).

⁶C. Lea and R. Gomer, Phys. Rev. Letters **25**, 804 (1970); J. W. Gadzuk and E. W. Plummer, *ibid.* **26**, 92 (1971).

⁷F. Forstmann and V. Heine, Phys. Rev. Letters **24**, 1419 (1970); F. Forstmann and J. B. Pendry, Z. Physik

235, 75 (1970).

⁸E. W. Plummer and J. W. Gadzuk, Phys. Rev. Letters **25**, 1493 (1970).

⁹E. W. Plummer and C. E. Kuyatt, Rev. Sci. Instr. (to be published).

¹⁰R. H. Good and E. W. Müller, in *Handbuch der Physik*, edited by S. Flügge (Springer, Berlin, 1956), Vol. **21**, p. 176.

¹¹S. C. Miller and R. H. Good, Jr., Phys. Rev. **91**, 174 (1953).

¹²E. L. Murphy and R. H. Good, Jr., Phys. Rev. **102**, 1464 (1956).

¹³S. G. Christov, Phys. Status Solidi **17**, 11 (1966).

¹⁴H. Neumann, Physica **44**, 587 (1969).

¹⁵C. B. Duke, *Tunneling in Solids* (Academic, New York, 1969), pp. 30-36.

¹⁶R. D. Young and H. E. Clark, Phys. Rev. Letters

17, 567 (1966); Appl. Phys. Letters 9, 265 (1966).

¹⁷R. G. Sachs and D. L. Dexter, J. Appl. Phys. 21, 1304 (1950).

¹⁸P. H. Cutler and J. J. Gibbons, Phys. Rev. 111,

394 (1958).

¹⁹P. H. Cutler and R. H. Good, Jr., Phys. Rev. 104, 308 (1956).

PHYSICAL REVIEW B

VOLUME 3, NUMBER 7

1 APRIL 1971

Excited-State Absorption Cross Sections for the Cr^{3+} Ion in MgO and Spinel

R. M. Macfarlane

IBM Research Laboratory, San Jose, California 95114

(Received 6 November 1970)

We have calculated numerically the magnetic dipole absorption cross sections for the excited-state transitions $t_2^3 {}^2E \rightarrow t_2^3 {}^2T_2$ and $t_2^3 {}^2T_1 \rightarrow t_2^3 {}^2T_2$ in centrosymmetric $\text{MgO}:\text{Cr}^{3+}$ and $\text{MgAl}_2\text{O}_4:\text{Cr}^{3+}$. This was done by using a parametrized ligand-field model in which the parameters are determined by the zero-field energies. The dominant contribution to the ${}^2E \rightarrow {}^2T_2$ absorption comes from Coulomb admixture of $t_2^3 e$ and $t_2^3 t_2$ terms, whereas the spin-orbit interaction contributes substantially to the ${}^2T_1 \rightarrow {}^2T_2$ cross section. The values obtained provide a reliable guide to the assignment of recent ${}^2E \rightarrow {}^2T_2$ excited-state absorption measurements in $\text{MgO}:\text{Cr}^{3+}$.

I. INTRODUCTION

The measurement of absorption from excited metastable states in solids is becoming an important spectroscopic technique. One of the main reasons for this is that it enables the observation of excited states which may be forbidden or only weakly allowed in transitions from the ground state. For example, transitions from the $t_2^3 {}^4A_2$ ground state of d^3 impurity ions (e.g., Cr^{3+}) to other nominally t_2^3 levels (2E , 2T_1 , and 2T_2) are essentially spin forbidden and derive their intensity from spin-orbit admixture of $t_2^3 e$ and $t_2^3 t_2$. On the other hand, transitions within the doublet terms are spin allowed and have much higher cross sections than those from the ground state. When the impurity-ion site lacks a center of symmetry, the absorption will, almost always, be electric dipole (ED) due to the admixture of odd-parity states into the d -like states. On the other hand, for ions in centrosymmetric sites where ED transitions are forbidden, the zero-phonon lines will be much weaker and magnetic dipole (MD) in nature. A number of experimental studies of excited-state absorption have been made, almost all on ruby ($\text{Al}_2\text{O}_3:\text{Cr}^{3+}$),¹⁻⁸ where the Cr^{3+} site is not centrosymmetric. In this case, the zero-phonon lines are electric dipole and have been definitely identified only for the $t_2^3 {}^2E$, ${}^2T_1 \rightarrow {}^2T_2$ transitions,³⁻⁵ which have an integrated absorption coefficient per ion of about 10^{-17} cm (oscillator strength $f = 5 \times 10^{-6}$). Tentative assignments of the zero-phonon transitions ${}^2E \rightarrow {}^2A_1$ and 2A_2 have also been made.⁸

A theoretical calculation of ED absorption cross sections is difficult because of a lack of knowledge

of the detailed nature of the odd-parity states involved and of the odd-parity crystal field. Thus in the perturbation treatment by Shinada *et al.*,⁶ the excited-state absorption coefficients in ruby are obtained in terms of a number of unknown parameters, which are the reduced matrix elements of the odd-parity crystal field (which produces the mixing leading to the ED transitions). This means that the relative absorption strengths cannot be calculated uniquely, and the absolute strengths can only be roughly estimated.

The complications outlined above for ED calculations do not arise for MD absorption which is parity allowed within the d^3 configuration. We report here the first numerical calculation of MD excited-state absorption coefficients. By transforming the MD operator to the basis of the eigenvectors of the impurity Hamiltonian [Eq. (1)], we have obtained absolute absorption coefficients for the $t_2^3 {}^2E_g \rightarrow t_2^3 {}^2T_{2g}$ and $t_2^3 {}^2T_{1g} \rightarrow t_2^3 {}^2T_{2g}$ transitions for two centrosymmetric $3d^3$ systems, viz., Cr^{3+} in the cubic sites of MgO , and Cr^{3+} in the trigonal sites of spinel (MgAl_2O_4 or ZnAl_2O_4). The only parameters involved are those determining the zero-field energies and g values, and these can be overdetermined without reference to experimental intensity measurements. We find that the integrated absorption coefficient per ion for the $t_2^3 {}^2E_g \rightarrow {}^2T_{2g}$ transition is $\approx 10^{-19}$ cm ($f = 5 \times 10^{-8}$). Reliable analytical perturbation expressions for the MD intensities cannot be obtained. In Sec. II the dependence of the MD line strengths on the zero-field parameters is explored, and it is found that the $t_2^3 {}^2E \rightarrow {}^2T_2$ strength is almost independent of trigonal and spin-orbit